Redox graft polymerization of vinylic monomers on ozone-activated poly(styrene-divinylbenzene) microspheres of narrow size distribution

Eran Partouche and Shlomo Margel*

Received (in Gainesville, FL, USA) 11th July 2007, Accepted 14th September 2007
First published as an Advance Article on the web 1st October 2007
DOI: 10.1039/b710584c

Uniform micrometer-sized polystyrene/poly(styrene-divinylbenzene) composite particles were produced by a single-step swelling of polystyrene template microspheres with styrene, divinylbenzene and benzoyl peroxide, followed by polymerization of the monomers within the swollen particles at 70 °C. Uniform crosslinked poly(styrene-divinylbenzene) microspheres of high surface area were then produced by dissolution of the polystyrene template part of the former composite particles. Hydroperoxide-conjugated microspheres were produced by ozonolysis of the crosslinked poly(styrene-divinylbenzene) particles. Redox graft polymerization of acrylonitrile and chloromethylstyrene on the hydroperoxide-conjugated particles was then accomplished. The influence of various polymerization parameters on the grafting yield was elucidated. Uniform polyaldehyde microspheres were produced from the former particles in two ways: (1) $LiAlH_4$ reduction of the nitrile groups of the polyacrylonitrile-grafted particles, followed by reaction of the formed primary amino groups with glutaraldehyde; (2) Sommelet reaction on the polychloromethylstyrene-grafted particles. Trypsin was then covalently bound to the polyaldehyde-grafted microspheres. A comparison between the enzymatic activity of the conjugated and free trypsin was accomplished.

Introduction

Micrometer-sized particles of narrow size distribution have attracted much attention in many applications such as adsorbents for high-pressure liquid chromatography, calibration standards, spacers for liquid crystals, inks, catalysis, and so forth.[1–7] Dispersion polymerization is the common method for preparing uniform non-porous micrometer-sized particles in a single step.[8–11] However, the particles formed by this method possess a relatively small surface area and their properties, *e.g.*, porosity, surface morphology and functionality, can hardly be manipulated.[8,11] Furthermore, uniform particles of a diameter larger than 5 μm usually cannot be prepared by dispersion polymerization. An alternative method for synthesis of uniform non-porous and porous polydivinylbenzene microspheres of sizes up to approximately 7 μm based on the precipitation polymerization technique in acetonitrile was reported by Stöver and co-workers.[12–16] Other alternative techniques to overcome the previous described limitations are based on several swelling methods of polystyrene (PS) template particles (formed by emulsion or dispersion polymerization) with appropriate monomers and initiators, *e.g.* multi-step swelling,[17–23] dynamic swelling,[24,25] and a single-step swelling,[26] followed by polymerization of the monomers within the swollen template particles.

There is much interest among the academic and industrial scientific communities in finding new ways to modify the surface of micrometer-sized particles without changing their bulk properties. The reasons for seeking this kind of modification are many, *e.g.* changing the surface composition and wettability properties, improving adhesion, protein and enzyme immobilization, blood compatibility, weathering, protection of particles, *etc.*[27–31] Numerous methods for surface modification of different particles such as high-energy radiation (*e.g.* gamma, glow discharge, corona discharge or photo-irradiation),[32] ozone exposures,[31,33] graft polymerization on core particles,[16] *etc.*, have been published.

The present article describes a simple method for surface modification and functionalization of crosslinked poly(styrene-divinylbenzene) [P(S-DVB)] micrometer-sized particles of narrow size distribution by ozonolysis, followed by radical graft polymerization of appropriate vinylic monomers. Previous studies with PS powder and PS dissolved in organic solvents, as well as with other polymers (*e.g.* polypropylene, polyethylene, polyethylene terephthalate and polyurethane), demonstrated the generation of several oxygen-containing groups, such as hydroperoxides, ketones and acids, as a consequence of their exposure to ozone.[34–36]

Recent studies in our research group described graft polymerization at 70 °C of vinylic monomers on ozone-oxidized P(S-DVB) particles.[37] The present article describes a simplification process through which redox graft polymerization at room temperature of vinylic monomers such as acrylonitrile (AN) and chloromethylstyrene (CMS) on hydroperoxide-conjugated crosslinked P(S-DVB) particles was accomplished. The influence of various polymerization parameters, *e.g.* $NaHSO_3$, monomer and conjugated hydroperoxide concentrations, on the grafting yield was elucidated. The

Department of Chemistry, Bar-Ilan University, Ramat-Gan, 52900, Israel. E-mail: shlomo.margel@mail.biu.ac.il. E-mail: ch190@mail.biu.ac.il; Fax: 972-3-6355208; Tel: 972-3-5318861

polyacrylonitrile (PAN) and polychloromethylstyrene (PCMS)-grafted particles were then used for the preparation of polyaldehyde particles. The aldehyde groups of these particles were used for binding proteins such as trypsin *via* the formation of Schiff-base bonds. This interaction of the trypsin and the polyaldehyde microspheres may be performed in a single-step and under physiological, or close to physiological pH[38–40] The concentration of the bound trypsin, binding efficiency, and the enzymatic activity of the immobilized trypsin relative to free trypsin were also elucidated.

Experimental

Chemicals

The following analytical-grade chemicals were purchased from Sigma-Aldrich, and were used without further purification: trypsin type IX from bovine pancreas (16 300 units mg^{-1} protein), α_1-antitrypsin from human plasma, *N*-α-benzoyl-L-arginine ethyl ester hydrochloride (BAEE), acetic acid *N*-hydroxysuccinimide ester (NHS), phosphate buffer (PB, 0.1 M, pH 7.4), phosphate buffer saline (PBS, 0.1 M, pH 7.4), bicarbonate buffer (BB, 0.1 M, pH 8.3), sodium cyanoborohydride (>95%), hexamethylenetetramine (HMTA), potassium bromide, potassium and sodium iodide, acetic acid (AcOH), HCl (36% and 1 M), NaOH (1 M), isopropanol (ISP), ethanol (HPLC), acetonitrile (99.9%), *N*,*N*-dimethylformamide (DMF, 99.9%), dibutyl phthalate (DBP, 99.9%), anhydrous diethyl ether (>99.7%), sodium metabisulfite (97%), hydroxylamine hydrochloride (98%), $LiAlH_4$ (95%), ethanolamine (99.5%), glutaraldehyde (GA, 25 wt% solution in water), PAN (MW 86 200) and benzoyl peroxide (BP, 98%). Styrene (99%), divinylbenzene (DVB, 80%) and CMS (99%) were passed through an activated alumina (ICN) to remove the inhibitor before use. AN was distilled before use. Water was purified by passing deionized water through an Elgastat Spectrum reverse osmosis system (Elga Ltd, High Wycombe, UK). Ozone was produced by passing a current of oxygen through a corona discharge (Ozomax. Canada) at voltages from 4.5 to 9 kV.

Synthesis of uniform PS template microspheres

PS template microspheres of 2.2 ± 0.2 μm were prepared according to the literature.[8,10,37]

Synthesis of uniform micrometer-sized PS/P(S-DVB) composite particles by a single-step swelling process

Uniform micrometer-sized PS/P(S-DVB) composite particles of 5.0 ± 0.4 μm were formed by a single-step swelling of the PS template particles with emulsion droplets of DBP containing styrene, DVB, and BP, followed by polymerization of the monomers within the swollen particles at 70 °C, according to the literature.[37]

Synthesis of uniform micrometer-sized crosslinked P(S-DVB) particles

Uniform crosslinked micrometer-sized P(S-DVB) particles were prepared by dissolving the PS template polymer of the PS/P(S-DVB) composite particles with DMF. Briefly, 500 mg of PS/P(S-DVB) composite particles dispersed in 30 mL of DMF were shaken at room temperature for *ca.* 12 h. The dispersed particles were then centrifuged, and the supernatant containing the dissolved PS template polymer was discarded. The crosslinked P(S-DVB) particles were then washed by intensive centrifugation cycles with DMF, water and ethanol. The crosslinked particles were then dried in a vacuum oven. Light scattering measurements indicate that the size and size distribution of the P(S-DVB) particles remained the same as before the dissolution of the PS part.

Synthesis of oxidized uniform micrometer-sized crosslinked P(S-DVB) particles

400 mg of crosslinked micrometer-sized P(S-DVB) particles dispersed in 20 mL pure water were introduced into a 250 mL round bottom flask. An O_3/O_2 stream containing an ozone output of 4 g h^{-1} was bubbled through the dispersed particles at room temperature for 30 min at a flow rate of 1.0 L min^{-1}. The oxidized particles were then washed free of excess ozone by intensive centrifugation cycles with water, until the supernatant did not show any indication of free ozone, as measured spectrophotometrically with KI.[41] These measurements indicated that the conjugated hydroperoxide concentration was 0.8 mmol g^{-1} particles. Particles containing different conjugated hydroperoxide concentrations were prepared by controlling the ozonolysis time period.

Redox graft polymerization of AN and CMS on the oxidized crosslinked P(S-DVB) microspheres

In a 15 mL pressure tube (Aldrich), 100 mg of the oxidized crosslinked micrometer-sized P(S-DVB) particles were dispersed in 5 mL of acetonitrile containing different concentrations of AN or CMS. 400 μL of an aqueous solution containing 0.4 mmol sodium metabisulfite were then added to the former dispersion. Graft polymerization of the vinylic monomers on the oxidized particles was accomplished by shaking the sealed pressure tube at room temperature for 22 h. The formed P(S-DVB)/PAN and P(S-DVB)/PCMS grafted composite particles were then washed by intensive centrifugation cycles with DMF, water and ethanol, respectively. The grafted particles were then dried in a vacuum oven. The influence of various polymerization parameters, *e.g.* sodium metabisulfite, monomers and conjugated hydroperoxide concentrations on the grafting yield, was elucidated.

Synthesis of uniform micrometer-sized polyaldehyde particles

Microspheres containing aldehyde groups were prepared in two ways: (1) reduction of the nitrile groups on the PAN-grafted particles,[42] followed by the reaction of the formed primary amino groups with GA; (2) Sommelet reaction[43] on the PCMS-grafted particles.

Method 1. 200 mg (2.3 mmol nitrile groups) of dried P(S-DVB)/PAN composite particles (prepared by the graft polymerization of 70% AN on the P(S-DVB) particles) were added gradually to a stirred mixture at 4 °C containing 133.3 mg (3.5 mmol) $LiAlH_4$ and 4 mL dry diethyl ether. Then, the resultant mixture was heated under reflux at 43 °C for 0.5 and 6.0 h, in order to produce particles containing two

different primary amine concentrations. The excess of $LiAlH_4$ was then quenched by gradually adding 2 mL water to the reaction mixture stirred at 4 °C, followed by 7 mL HCl (1 M). The formed poly(styrene-divinylbenzene)/polyallylamine composite microspheres [P(S-DVB)/PAA1 and P(S-DVB)/PAA2—low and higher primary amine particles, respectively] were washed by intensive centrifugation cycles with NaOH (1 M) and water, and then dried by lyophilization. Polyaldehyde particles were formed by interacting the aminated P(S-DVB)/PAA composite particles with GA according to the literature.[42] Briefly, 70 mg of the P(S-DVB)/PAA composite microspheres were added to a 5 mL conical vial containing 1.7 mL GA (12.5%) in BB (pH 8.3). The mixture was then shaken at room temperature for *ca.* 12 h. Sodium cyanoborohydride (*ca.* 4 mg) was then added to the shaken dispersion for an additional 4 h. The formed aldehyde-modified microspheres [P(S-DVB)/PAA-GA], were then washed by intensive centrifugation cycles with PBS. Residual primary amino groups were then blocked by adding 35 mg NHS to the P(S-DVB)/PAA-GA composite particles dispersed in 10 mL PBS. The mixture was then shaken at room temperature for 2 h. The polyaldehyde composite particles were then washed by intensive centrifugation cycles with water, and then dried by lyophilization.

Method 2. 6.2 mL of AcOH and 0.93 mg of HMTA were added to a 6.2 mL aqueous dispersion containing 400 mg of the crosslinked P(S-DVB)/PCMS composite particles. The resultant mixture was stirred under reflux (100 °C) for 22 h. 7.5 mL of concentrated HCl (36%) were then added to the reaction mixture at room temperature, and the mixture stirred for an additional 20 min. The formed aldehyde-modified poly(styrene-divinylbenzene)/poly(vinyl benzaldehyde) composite particles [P(S-DVB)/PVBA] were washed by intensive centrifugation cycles with water, and then dried by lyophilization.

Trypsin immobilization on the uniform micrometer-sized polyaldehyde particles

8 mg of trypsin were added to a 15 mL PP tube containing 20 mg of P(S-DVB)/PAA-GA or P(S-DVB)/PVBA composite particles dispersed in 10 mL BB (pH 8.3). The mixture was then shaken at room temperature for 22 h. Unreacted aldehyde groups were then blocked by adding to the shaken mixture 2 mL ethanolamine BB solution (0.1%). This mixture was then shaken at room temperature for an additional 12 h. The trypsin-immobilized composite particles [P(S-DVB)/PAA-GA-trypsin and P(S-DVB)/PVBA-trypsin] were then washed from unbound trypsin and ethanolamine by intensive centrifugation cycles with PBS (pH 7.4).

Analysis

Size and size distribution. The diameter and size distribution of the various microspheres dispersed in the aqueous phase were determined by a micron particle analyzer, model LS100, Coulter Electronics. The reported values are an average of at least four replications of each measurement.

Conjugated hydroperoxide content. The conjugated-hydroperoxide concentration was determined according to Carlsson and Wiles.[44] Briefly, 20 mL of a NaI/ISP (14 g/100 mL) solution and 70 mL of a AcOH–ISP (1 : 10 v/v) solution were introduced into a 250 mL round bottom flask containing 100 mg of the oxidized P(S-DVB) crosslinked particles. After 30 min reflux, the suspension was cooled to room temperature, and 10 mL of pure water was added. The particles were then separated from the supernatant by centrifugation. The I_3^- concentration in the supernatant (formed due to the decomposition of the conjugated hydroperoxides by I^-) was determined by a Cary-1E UV-visible spectrometer at 360 nm, through a calibration curve.

% Grafting. The grafting yield of PAN and PCMS on the micrometer-sized crosslinked P(S-DVB) particles was measured according to the following equations:

$$\%\ \text{Grafted PAN} = (\%\ N_{exptl}/\%\ N_{theor}) \times 100 \qquad (1)$$

$$\%\ \text{Grafted PCMS} = (\%\ Cl_{exptl}/\%\ Cl_{theor}) \times 100 \qquad (2)$$

The % N_{exptl} and Cl_{exptl} was measured by elemental analysis

Primary amine content. The primary amine content of the P(S-DVB)/PAA composite particles was determined by two ways: (1) Spectrophotometrically at 570 nm according to the ninhydrin assay, as described in the literature;[45,46] (2) measuring the relative decrease of the FTIR nitrile absorption peak at *ca.* 2243 cm^{-1} due to the reduction of the nitrile groups by $LiAlH_4$.

Aldehyde content. The aldehyde content of the P(S-DVB)/PVBA composite particles was also measured in two ways: (1) Measuring the relative decrease of the FTIR C–Cl absorption peak at *ca.* 1265 cm^{-1} due to the Sommelet reaction, which converts each chloride group to aldehyde; (2) calculations based on the % nitrogen of the oxime groups formed as a result of the reaction between the aldehydes and hydroxylamine hydrochloride, according to the literature.[38] Briefly, 100 mg hydroxylamine hydrochloride was added to a 15 mL PP tube containing 10 mg of P(S-DVB)/PVBA dispersed in 10 mL of pure water. The tube was then sealed and shaken at room temperature for 22 h. The oxime microspheres were then washed by intensive centrifugation cycles with water, and dried by lyophilization. The % nitrogen of the oxime groups was determined by elemental analysis and the aldehyde concentration was then calculated, respectively. It should be noted that the aldehyde content of the P(S-DVB)/PAA-GA particles could not be measured similarly due to the insignificant difference between the nitrogen content of the P(S-DVB)/PAA-GA and its oxime adduct.

Trypsin binding. The concentration of the immobilized trypsin was measured spectrophotometrically at 650 nm according to the Lowry method.[47]

Trypsin activity. The activity of the free and immobilized trypsin against BAEE was determined according to Boyer.[48] (One unit (U) of trypsin with BAEE produced a change in A_{253} of 0.001 min^{-1} at pH 7.5, 25 °C in a volume of 3 mL). A known amount of dried immobilized trypsin particles was

added to a 13 × 100-mm glass tube containing 2.6 mL of PB (0.1 M, pH 7.4). 0.4 mL of the substrate solution (1.9 mg BAEE/mL PB) was then added, and the mixture was shaken at room temperature for 7 min. The trypsin-conjugated particles were then precipitated by centrifugation, and the supernatant was analyzed spectrophotometrically at 253 nm. A similar procedure substituting the immobilized trypsin with free trypsin was performed in order to determine the activity of free trypsin towards BAEE. Inhibition of the free- and the trypsin-immobilized particles was accomplished by adding various concentrations of α_1-antitrypsin to 13 × 100-mm glass tubes containing fixed amounts of free or immobilized trypsin dispersed in 2.6 mL PB (0.1 M, pH 7.4). The mixture was then shaken at room temperature for 10 min. The activity of the α_1-antitrypsin-inhibited free or conjugated trypsin was then measured with BAEE according to the previously described procedure. (8.6 mg α_1-antitrypsin will inhibit one mg trypsin with an activity of 10 000 BAEE units mg^{-1} proteins).

Equipment

Elemental analysis. The elemental analysis of the various particles was performed using an elemental analysis instrument; model EA1110, CE Instruments, Thermoquast.

XPS. Surface elemental analysis was obtained by X-ray photoelectron spectroscopy (XPS), model AXIS-HS, Kratos Analytical, England, using Al-Kα lines, at 10^{-9} Torr, with a take-off angle of 90°. Both the XPS and elemental analysis reported values are the average of measurements performed on at least three samples and have a maximum error of about 10 and 2%, respectively.

SEM. SEM surface images were taken using a JEOL, JSM-840 model, Japan. Samples for SEM were prepared by placing a drop of the diluted sample on a glass plate, followed by vapor-deposition of a thin layer of gold on the particles mounted on the glass plate.

TEM. Cross-section pictures of the microspheres were characterized with a JEOL JEM-1200EX Transmission Electron Microscope (TEM). Microspheres were embedded in Spurr's epoxy, sectioned with an ultratome, and then viewed with the TEM. Dyeing was not necessary for the TEM visualization.

BET. The surface area of the various particles was measured by the Brunauer–Emmet–Teller (BET) method,[49] Gemini III model 2375, Micrometrics.

TGA–DSC. The thermal behavior of the various particles was measured by thermogravimetric analysis (TGA) and differential scanning calorimetry (DSC). The analysis was performed with a TC15 system equipped with TGA, model TG-50 and DSC, model DSC-30, Mettler Toledo. The analysis was performed with dried samples of about 5 mg in a dynamic nitrogen atmosphere (200 mL min^{-1} for TGA and 50 mL min^{-1} for DSC) with a heating rate of 10 °C min^{-1}.

FTIR. Fourier Transform Infrared (FTIR) analysis was performed with a Bomem FTIR spectrophotometer; model MB100, Hartman & Braun. The analysis was performed with 13 mm KBr pellets that contained 2 mg of the detected material and 198 mg of KBr. The pellets were scanned over 200 scans at a 4 cm^{-1} resolution.

Results and discussion

In this study, ozone-induced grafting was used for the surface modification and functionalization of uniform crosslinked P(S-DVB) microspheres formed by a single-step swelling process of PS template particles.[26,50] The P(S-DVB) microspheres were oxidized by bubbling ozone through an aqueous dispersion containing these particles. This treatment commonly results in the degradation of the P(S-DVB),[41] and in the formation of several oxygen-containing groups conjugated to the particles, *e.g.* hydroperoxides.[37] These conjugated hydroperoxides have been used in this study as initiators for the redox graft polymerization of AN and CMS onto the crosslinked P(S-DVB) particles. The special features of such a graft polymerization are a very short induction period, a relatively low energy of activation, and the low temperature required. A literature search has revealed that various peroxide/sodium metabisulfite redox pairs are very common in water.[51,52] Bajpai and co-workers proposed that the reductant in the aqueous redox polymerization of acrylamide using potassium permanganate/sodium metabisulfite as redox initiator, is the bisulfite anion (HSO_3^-), which is in equilibrium with metabisulfite anion.[53] Ebdon *et al.* also supported the idea that the reducing part of this redox pair in the polymerization of acrylonitrile initiated by ammonium persulfate/sodium metabisulfite redox pair is the bisulfite anion.[54] The addition of an aqueous solution of sodium metabisulfite to the hydroperoxide-conjugated crosslinked P(S-DVB) particles dispersed in acetonitrile results in the breakage of the hydroperoxide groups to form alkoxyl radicals, bisulfite radicals and hydroxyl ions. In the presence of appropriate vinylic monomers such as AN and CMS, the conjugated alkoxyl radicals initiate the graft polymerization, while the bisulfite radicals may initiate homopolymerization. The homopolymers of PAN and PCMS were removed from the graft polymers by intensive washing of the grafted particles with DMF.

Hydrodynamic diameter of PS, PS/P(S-DVB) and P(S-DVB) microspheres

Fig. 1 demonstrates the hydrodynamic diameter and size distribution of the PS template particles (Fig. 1(A)) and the crosslinked P(S-DVB) particles (Fig. 1(B)). This figure indicates a single population for both particles: 2.2 ± 0.2 μm for the PS template microspheres and 5.0 ± 0.4 μm for the crosslinked particles. It should be noted that the histograms of the PS/P(S-DVB) composite particles and the oxidized crosslinked P(S-DVB) particles illustrated the same average diameter and size distribution as that of the crosslinked P(S-DVB) particles.

Ozonolysis of the crosslinked P(S-DVB) microspheres

Extensive study was done to estimate the optimal ozonolysis duration on the crosslinked P(S-DVB) microspheres.[37] It was found that the longer the ozonolysis duration, the higher is the concentration of the conjugated hydroperoxide groups. On the

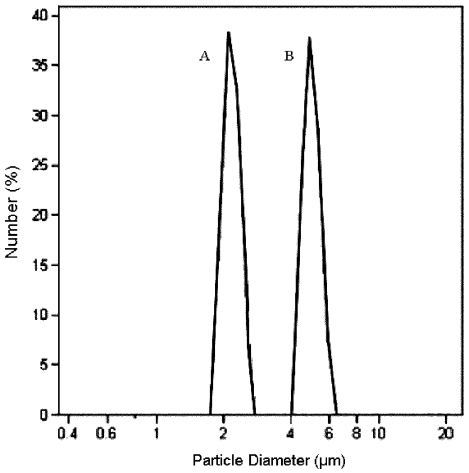

Fig. 1 Particle-size histograms of the PS template microspheres (A) and the crosslinked P(S-DVB) microspheres (B). PS and P(S-DVB) particles as prepared according to the Experimental section.

other hand, longer ozonolysis duration caused morphology damage and a drop in the mechanical properties of the particles due to degradation processes. The optimal ozonolysis duration in this study was set up to 30 min, yielding 0.8 mmol of conjugated hydroperoxides g^{-1} microspheres, so that sufficient hydroperoxide groups for the graft polymerization were obtained with minimal mechanical damage to the P(S-DVB) microspheres.[37] Fig. 2(A) and (B) illustrate by a SEM image and a cross-section TEM image, respectively, the narrow size distribution and the porous structure of the oxidized crosslinked particles. BET measurements, as shown in Table 1, confirm the porous structure of these crosslinked particles by demonstrating a significantly higher surface area of these particles compared to the calculated surface area of nonporous particles of similar average diameter, 89.3 and 1.2 m^2 g^{-1}, respectively.

Redox graft polymerization of AN and CMS on the oxidized crosslinked P(S-DVB) microspheres

Graft polymerization of AN and CMS on the crosslinked P(S-DVB) microspheres was initiated by the conjugated alkoxyl radicals generated by adding 400 μL of an aqueous solution of $NaHSO_3$ (formed by the decomposition of sodium metabisulfite in water) to the hydroperoxide-conjugated particles dispersed in 5 mL of acetonitrile. The homopolymers of

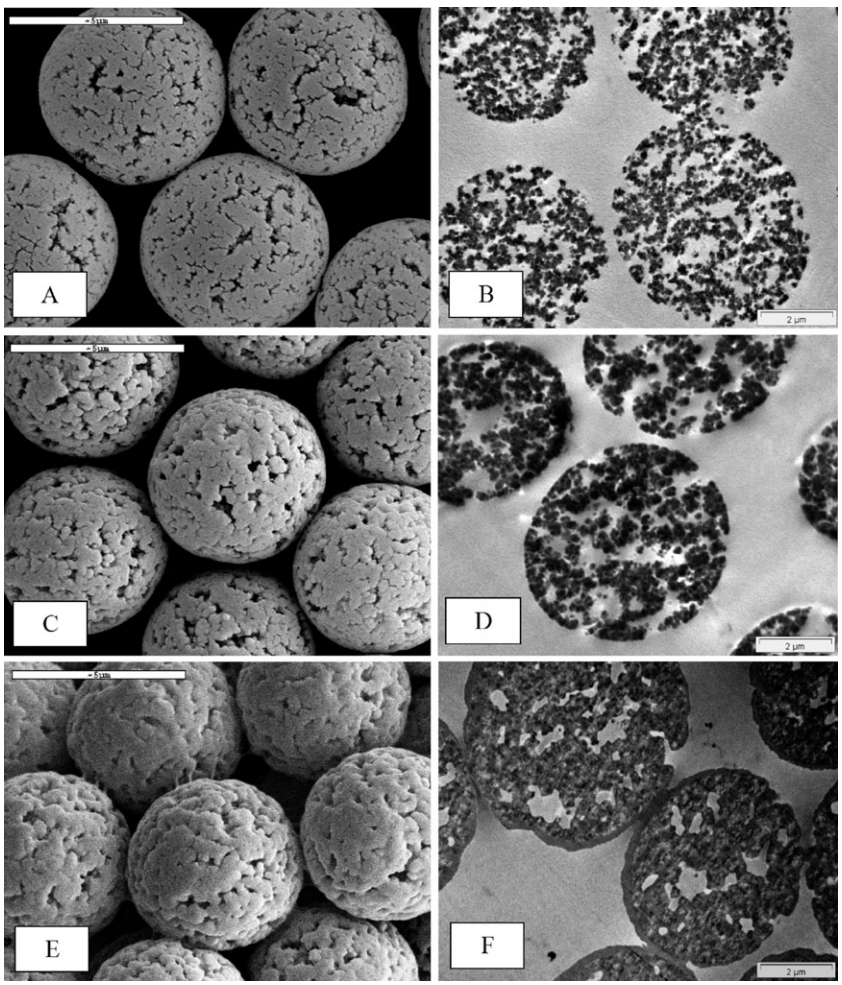

Fig. 2 SEM and cross-section TEM images of the oxidized crosslinked P(S-DVB) microspheres before (A and B) and after graft polymerization of AN (C and D) and CMS (F and E), respectively. Graft redox polymerization of the monomers was performed according to the experimental section in the presence of 70% (v/v) monomer initial concentration.

Table 1 Mean diameter, calculated and measured surface area of the oxidized P(S-DVB), P(S-DVB)/PAN and P(S-DVB)/PCMS particles[a]

		Surface area/m^2 g^{-1}	
Microspheres	Mean diameter/μm	Calc.	Found
Oxidized P(S-DVB)	5.0	1.2	89.3
P(S-DVB)/PAN	5.0	1.2	17.0
P(S-DVB)/PCMS	5.1	1.2	3.4

[a] Synthesis and ozonolysis of the particles were performed according to the experimental section. Graft polymerization of the monomers was also performed according to the Experimental section in the presence of 70% (v/v) monomers initial concentrations. [b] Calculated surface area is based on the assumption that the particles are non-porous spheres with density of 1.0 g cm^{-3}. The calculation was performed according to the following equation: $S = 6/Dd$, wherein S is the surface area (m^2 g^{-1}), D is the diameter (μm), and d is the density (g cm^{-3}) of the particles.

PAN and PCMS formed in the continuous phase (acetonitrile) by the bisulfite radicals were removed from the grafted polymers by intensive washing with DMF. A qualitative indication of the success of the graft polymerization of AN was observed by following the FTIR peak of the grafted particles at *ca.* 2243 cm^{-1} (nitrile stretching band) and for the CMS at *ca.* 1265 cm^{-1} (chloride stretching band). It is well known that redox polymerization is relatively inefficient in a sense that one does not generate a high concentration of radicals per mol of initiator. However, such an approach is followed only if one is not very concerned about the efficiency of this type of reaction, but rather with the ability to generate radical species under controlled temperature conditions.[55] Fig. 3 illustrates the % grafting yield of PAN and PCMS on the crosslinked P(S-DVB) particles as a function of the mol ratio of [$NaHSO_3$] : [conjugated hydroperoxides]. The % grafting yield was calculated as indicated in the Experimental section. Fig. 3 shows that at a [$NaHSO_3$] : [conjugated hydroperoxides] mol ratio of 1 : 1, the % grafting yield of PCMS is 19.9, and that of PAN is insignificant. This figure illustrates that the highest % grafting

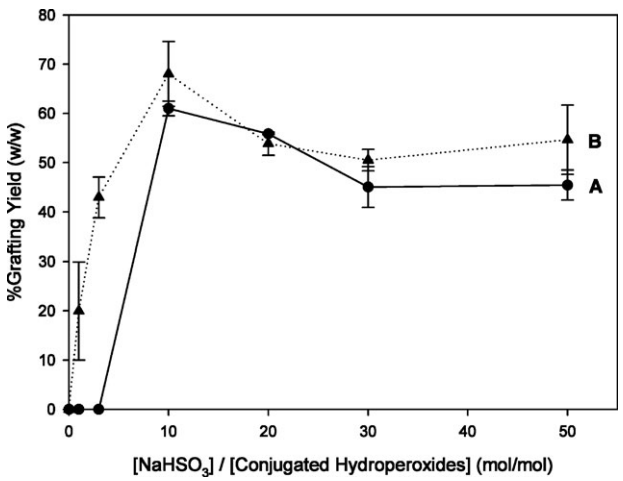

Fig. 3 % Grafting yield of PAN (A) and PCMS (B) as function of [$NaHSO_3$]/[conjugated hydroperoxides] mol ratio. Graft redox polymerization of the monomers was performed according to the experimental section in the presence of 70% (v/v) monomer initial concentrations.

Table 2 % Grafting yield of PAN and PCMS on the oxidized crosslinked P(S-DVB) microspheres as a function of the conjugated hydroperoxides concentration[a]

	% Grafting yield (w/w)	
[Hydroperoxide]/mmol g^{-1}	PAN	PCMS
0.8	18.0	53.3
1.5	25.0	71.6
2.2	26.0	75.2

[a] Synthesis and ozonolysis of the crosslinked P(S-DVB) particles were performed according to the Experimental section using different ozonolysis periods. The monomers grafting process was also performed according to the Experimental section in the presence of 30% (v/v) monomers initial concentrations and 0.4 mmol sodium metabisulfite.

yield of PAN and PCMS was accomplished at [$NaHSO_3$] : [conjugated hydroperoxides] mol ratio of 10 : 1—61.0 and 68.0%, respectively. Fig. 3 also illustrates that increasing the mol ratio of [$NaHSO_3$] : [conjugated hydroperoxides] above these maximal values leads to a consistent decrease in the % grafting yield of both monomers. This can account for the large number of radicals produced due to the high concentration of the $NaHSO_3$, thus promoting the termination processes.

Tables 2 and 3 demonstrate the % grafting of PAN and PCMS on the crosslinked P(S-DVB) microspheres as a function of conjugated hydroperoxides and monomer concentration, respectively. Table 2 illustrates that the grafting yield of PAN and PCMS on the crosslinked particles rises as the conjugated hydroperoxide concentration increases from 0.8 to 1.5 mmol g^{-1} particles. Thereafter, increasing the conjugated hydroperoxide concentration from 1.5 to 2.2 mmol g^{-1} scarcely affects the grafting yield. For example, the redox graft polymerization of AN or CMS in the presence of particles containing 0.8, 1.5 and 2.2 mmol g^{-1} results in a % PAN grafting of 18, 25 and 26, respectively, and a % PCMS grafting of 53.3, 71.6 and 75.2, respectively. It may be that hydroperoxide concentration above 1.5 mmol g^{-1} does not significantly affect the grafting yield due to the steric hindrance of existing grafted polymeric chains to additional grafting. Table 3 shows that as the concentration of the monomers rises, so do the

Table 3 % Grafting yield of PAN and PCMS on the oxidized crosslinked P(S-DVB) microspheres as function of monomers concentration[a]

	% Grafting yield (w/w)	
% Monomer (v/v)	PAN	PCMS
10	3.3	29.6
30	18.0	53.3
50	44.6	58.6
70	61.0	68.0
90	67.8	78.3

[a] Synthesis and ozonolysis of the crosslinked P(S-DVB) particles were performed according to the Experimental section. Graft polymerization of the monomers was also performed according to the Experimental section in the presence of 0.08 mmol/100 mg conjugated-hydroperoxide concentration, 0.4 mmol sodium metabisulfite and various initial monomer concentrations.

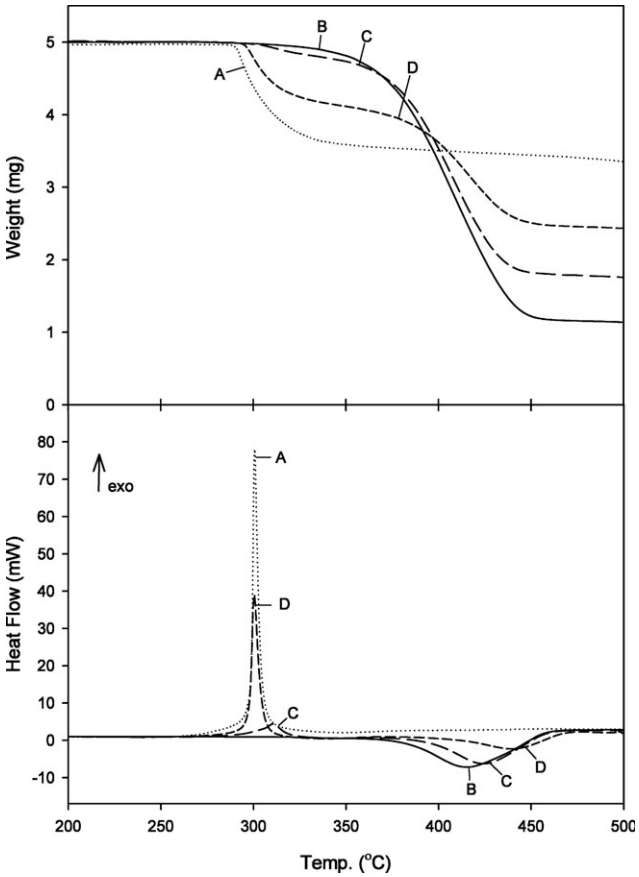

Fig. 4 TGA and DSC thermograms of commercial PAN powder (A) and various % of PAN grafted P(S-DVB) microspheres (B–D) formed by graft redox polymerization in the presence of 10, 30 and 70% (v/v) AN, respectively. Graft polymerization was performed according to the experimental section.

grafting yield. For example, redox graft polymerization of 10, 30, 50, 70 and 90% (v/v) AN or CMS in acetonitrile results in a % PAN grafting yield of 3.3, 18.0, 44.6, 61.0 and 67.8, respectively, and a % PCMS grafting yield of 29.6, 53.3, 58.6, 68.0 and 78.3, respectively.

Fig. 4 shows typical TGA (top) and DSC (bottom) thermograms of the commercial PAN powder (curve A) and PAN-grafted crosslinked P(S-DVB) microspheres obtained by the redox graft polymerization of various initial concentrations of AN: 10 (curve B), 30 (curve C) and 70% (curve D). The TGA curve of the PAN powder (curve A) exhibits a sharp weight loss (27%) between 290 and 320 °C. This weight loss resulted from the release of volatile compounds such as HCN, N_2, *etc.*, due to the cyclization of the PAN chains, as reported in the literature.[56] Increasing the temperature of the PAN beyond 550 °C up to 900 °C (not shown in Fig. 4) resulted in a mild total weight loss of *ca.* 50%, due to the carbonization of the PAN. The sharp weight loss between 290 to 320 °C is demonstrated by the DSC thermogram (curve A), by a sharp exothermic peak at 297 °C. The TGA of the PAN-grafted crosslinked P(S-DVB) microspheres (curves B–D) illustrate two slopes. The first slope indicates a weight loss resulting from the cyclization of the grafted PAN chains, while the second slope is due to a weight loss resulting from the decomposition of the crosslinked P(S-DVB) chains. This behavior is also confirmed by the DSC curves, by the exothermic peaks around 300 °C and the endothermic peaks around 415–440 °C, respectively. Curves B–D illustrate, as expected, that the weight loss (shown in the TGA curves) and the exothermic peaks (shown in the DSC curves) related to the cyclization of the PAN chains increase as long as the % PAN of the grafted particles rises. Curves B–D also demonstrate by both TGA and DSC that the decomposition temperature of the crosslinked P(S-DVB) chains increases as long as the % of grafted PAN of the P(S-DVB)/PAN rises. For example, Fig. 4 (curves B–D) shows that the decomposition exothermic peaks of the crosslinked P(S-DVB) chains related to the P(S-DVB)/PAN microspheres, prepared in the presence of 10, 30 and 70% AN initial concentrations, are 415, 424 and 440 °C, respectively. This shift towards higher decomposition temperatures as the % PAN of the composite particles increases may indicate a strong interaction between the P(S-DVB) and PAN chains (after cyclization).

Fig. 2(A), (C) and (E) display SEM images of the oxidized P(S-DVB) microspheres before (A) and after the graft polymerization of 70% AN (C) or CMS (E). The coating of the PAN and PCMS on the surface of the P(S-DVB) particles is clearly demonstrated by the increased surface roughness. The surface grafting by the PCMS chains is significantly higher than that observed by the PAN, as illustrated by the significant increase in the surface roughness of these particles.

Fig. 2(B), (D) and (F) display cross-section TEM images of the oxidized P(S-DVB) microspheres before (B) and after the graft polymerization of 70% AN (D) or CMS (F). These images reveal that these monomers polymerized not only on the P(S-DVB) outer surface, but also inside the internal pores of the particles. These pictures clearly illustrate that the pores are filled to a much higher extent by PCMS than by PAN, as also confirmed by the decreased surface area of these particles, *e.g.* 89.3, 17.0 and 3.4 $m^2\ g^{-1}$ for oxidized P(S-DVB), P(S-DVB)/PAN and P(S-DVB)/PCMS, respectively (see Table 1). Fig. 2 clearly illustrates that under similar polymerization conditions, the % grafting yield of PCMS is higher than that of the PAN. This result is also confirmed by Table 3, *e.g.* in the presence of 30 or 70% initial monomer concentrations the % grafting yield of PCMS on the P(S-DVB) microspheres is 53.3 and 68.0%, respectively, while that of the PAN is 18.0 and 61.0%, respectively. This difference in the graft polymerization yield of PCMS and PAN probably results from their hydrophobic traits, with respect to the P(S-DVB) particles. CMS, in contrast to AN, has a similar hydrophobic trait to that of the P(S-DVB) particles, and thereby its graft polymerization yield is significantly higher. Another possible explanation may be due to the significantly higher solubility of PCMS in acetonitrile relative to PAN.

Synthesis of polyaldehyde microspheres

(1) Synthesis of P(S-DVB)/PAA-GA microspheres. Primary amine-derivatized P(S-DVB)/PAN microspheres were prepared by the reduction of the nitrile groups of the P(S-DVB)/PAN particles with $LiAlH_4$. The reduction was performed for two different time periods in order to obtain

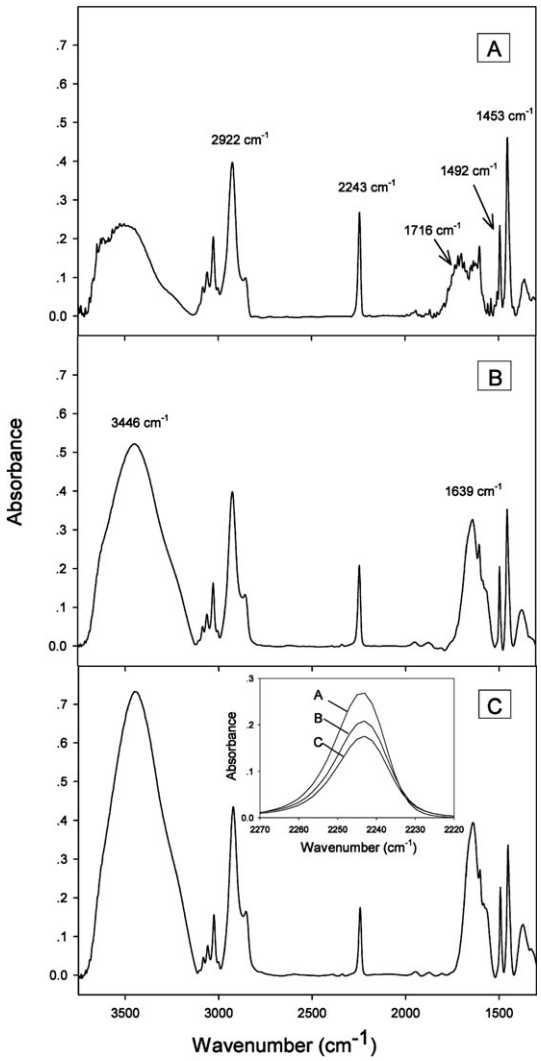

Fig. 5 FTIR spectra of P(S-DVB)/PAN microspheres (A), and P(S-DVB)/PAA microspheres produced by $LiAlH_4$ reduction of the P(S-DVB)/PAN particles for different time periods: 0.5 (B) and 6 h (C). The expansion illustrates the decrease in the nitrile absorbance peak as a consequence of the reduction duration. Graft polymerization was performed according to the Experimental section in the presence of 70% (v/v) AN initial concentration. Reduction of the nitrile groups of the PAN grafted particles was also performed according to the Experimental section.

particles derivatized with two different concentrations of amine groups. Fig. 5 depicts the FTIR spectra of the P(S-DVB)/PAN microspheres before (A) and after $LiAlH_4$ reduction for 0.5 (B) and 6.0 (C) h. The absorption peaks belonging to P(S-DVB)/PAN microspheres (Fig. 5(A)) at *ca.* 1453, 1492, 1507 and 3000–3100 cm^{-1} correspond to the aromatic –CH stretching bands; at *ca.* 2849 and 2922 cm^{-1} to $–CH_2–$; at *ca.* 1716 cm^{-1} to carbonyl formed by the ozonolysis process; and at *ca.* 2243 cm^{-1} to the nitrile of the grafted PAN. The reduction of the nitrile groups to primary amines leads to a decrease in the nitrile absorption peak at *ca.* 2243 cm^{-1}, and to the formation of N–H stretching and scissoring NH_2 at *ca.* 3446 and 1639 cm^{-1}, respectively. A quantitative ninhydrin assay for the determination of the active primary amine concentration indicated the formation of 0.15 and 0.24 mmol amines g^{-1} microspheres as a consequence of the nitrile reduction for 0.5 and 6 h, respectively. In contrast to the ninhydrin analysis, FTIR measurements, as shown by the expansion window of Fig. 5, indicate the formation of 1.91 and 2.90 mmol amines g^{-1} microspheres, respectively (assuming a complete reduction of the nitriles to amines). This difference may be explained by the reaction of the ninhydrin occurring only with the most accessible amines, contrary to the FTIR analysis, which related to the total amine content. It is important to mention that in spite of the fact that not all of the nitrile groups of the P(S-DVB)/PAN particles were reduced by $LiAlH_4$, we chose for simplicity to represent the reduced particles as P(S-DVB)/PAA. Polyaldehyde particles were prepared by binding GA to the amine-modified particles. The Schiff-base bonds thereby formed were then reduced by sodium cyanoborohydride to form the more stabilized C–N single bond. In order to prevent, as much as possible, the interaction of each GA molecule with two amino groups belonging to the same particle or to two neighboring particles, a large excess of GA (relative to the conjugated primary amine groups) was used (see Experimental section). FTIR measurements of the formed polyaldehyde microspheres could not detect aldehyde carbonyl bonds due to the low content of the aldehyde groups. Nevertheless, XPS studies indicated the formation of aldehyde groups as a consequence of the reaction of GA with the amine-modified particles, by the increase in the atomic concentration of oxygen belonging to the P(S-DVB)/PAA microspheres containing the low and higher primary amine content from 12.9 to 13.4% and from 16.2 to 23.8%, respectively. It should be noted that the presence of aldehyde groups was also confirmed by the reaction of these composite particles with trypsin, as will be described below. However, before the interaction of the polyaldehyde microspheres with trypsin, it was essential to block residual amine groups of the P(S-DVB)/PAA-GA microspheres in order to prevent non-specific interactions of the trypsin with the positively-charged primary amines. The blocking of residual amine groups was performed by interaction of the polyaldehyde particles with NHS, according to Scheme 1. The formation of amide bonds due to this interaction was sustained by XPS by the tail shown at 287 eV (Fig. 6(B)), which does not exist in the particles before interaction with NHS (Fig. 6(A)).

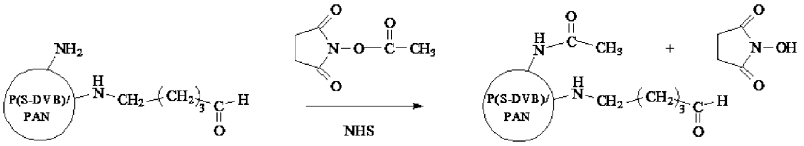

Scheme 1 A scheme illustrating the blocking of residual primary amine groups of P(S-DVB)/PAA-GA by NHS.

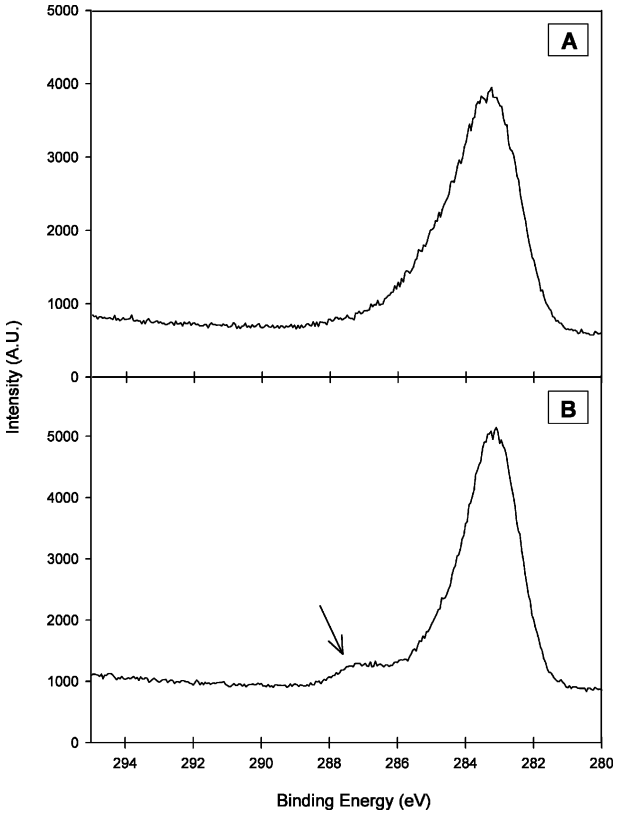

Fig. 6 XPS data of C 1s of P(S-DVB)/PAA2 microspheres before (A) and after blocking residual primary amines with NHS (B). The blocking reaction was performed according to the Experimental section.

(2) Synthesis of P(S-DVB)/PVBA microspheres. Conversion of the benzyl chloride groups belonging to the P(S-DVB)/PCMS microspheres to aldehyde groups by a single step was performed by the Sommelet reaction, as described in the Experimental section. The FTIR absorption peak at *ca.* 1739 cm^{-1} confirmed the aldehyde generation. The chloride concentration due to the Sommelet reaction decreased from 4.50 to 0.56 mmol chlorides g^{-1} microspheres (87.3% conversion). This result may indicate the formation of 4.4 mmol aldehydes g^{-1} microspheres, assuming that each chloride group converted to aldehyde. In contrast to the FTIR measurements, the aldehyde content measured by the nitrogen analysis of the oxime obtained by the reaction of the P(S-DVB)/PVBA microspheres with hydroxylamine, as described in the Experimental section, was 0.24 mmol aldehydes g^{-1} microspheres. This difference may again be explained by the reaction of hydroxylamine only with the most accessible aldehydes, contrary to the FTIR analysis, which related to the total aldehyde content of the particles.

Trypsin immobilization and activity

Trypsin was covalently bound to the polyaldehyde microspheres *via* the formation of polyvalent Schiff-base bonds (see Experimental section). In order to prevent side reactions between residual aldehyde groups and primary amine groups of the inhibitor α_1-antitrypsin, blocking the residual aldehyde groups after trypsin immobilization was performed with ethanolamine (see Experimental section). Table 4 compares the concentration of bound trypsin, binding efficiency, and the relative activity of the trypsin bound to the P(S-DVB)/PAA-GA and P(S-DVB)/PVBA microspheres. This table demonstrates that there are no significant differences in the bound trypsin nor in the binding efficiency of the two amine-modified particles namely, P(S-DVB)/PAA1 and P(S-DVB)/PAA2 in spite of the significant difference in their initial amine concentrations (as described previously). These results may indicate that the aldehyde content of these microspheres is not significantly different. Table 4 also shows that the concentration of the bound trypsin and the trypsin binding efficiency of the P(S-DVB)/PVBA microspheres is almost twice that of P(S-DVB)/PAA-GA. These results are expected, since the aldehyde content of the P(S-DVB)/PVBA microspheres is significantly higher than that of P(S-DVB)/PAA-GA (as was shown previously). Table 4 also illustrates that in spite of the two-fold bound trypsin, the relative % activity towards the BAEE of the trypsin bound to P(S-DVB)/PVBA microspheres (12.7%) is significantly lower than that bound to P(S-DVB)/PAA-GA (17.6%). This difference in trypsin enzymatic activity is not completely clear, and may be explained by steric hindrance to the activity of the denser trypsin particles. Table 4 also shows, as expected, that the covalent binding of trypsin to both particles P(S-DVB)/PAA-GA and P(S-DVB)/PVBA results in decreased activity relative to the free enzyme, *e.g.* the activity of the trypsin bound to P(S-DVB)/PAA-GA or P(S-DVB)/PVBA microspheres is only 17.6 and 12.7%, respectively, of that of the free enzyme. Usually, the covalent binding of enzymes to polymeric supports leads to a decrease in their activity, but, on the other hand, to an increase in their stability.[57,58] Indeed, free trypsin lost almost 100% of its activity towards BAEE upon storage at 4 °C of a free trypsin solution (1 mg mL^{-1}) in PB (0.1 M, pH 7.4). On the other hand, under similar conditions the trypsin bound to the particles [(P(S-DVB)/PAA-GA and P(S-DVB)/PVBA)] lost only 8% of its activity. Fig. 7 also demonstrates the stability of the bound trypsin compared to free trypsin in the presence of different concentrations of the α_1-antitrypsin inhibitor. Curve A in Fig. 7 illustrates the continuous activity loss as long as the [antitrypsin]/[trypsin] mol ratio increased from 1 to

Table 4 Bound trypsin, trypsin binding efficiency and trypsin relative activity of P(S-DVB)/PAA-GA-trypsin and P(S-DVB)/PVBA-trypsin particles compared to free trypsin[a]

Particles	Bound trypsin/μg trypsin mg^{-1} particles)	Trypsin binding efficiency (%)	Relative trypsin activity (%)
— (Free trypsin)	—	—	100.0
P(S-DVB)/PAA1-GA-trypsin	45.2	11.3	17.6
P(S-DVB)/PAA2-GA-trypsin	46.5	11.6	17.4
P(S-DVB)/PVBA-trypsin	94.0	23.5	12.7

[a] Synthesis, ozonolysis and trypsin immobilization were performed according to the Experimental section. Bound trypsin concentration was measured by the Lowry method;[47] Trypsin binding efficiency was calculated from the difference between the bound trypsin to the initial trypsin concentration; the relative trypsin activity against BAEE is related to that of free trypsin which considered as 100%.

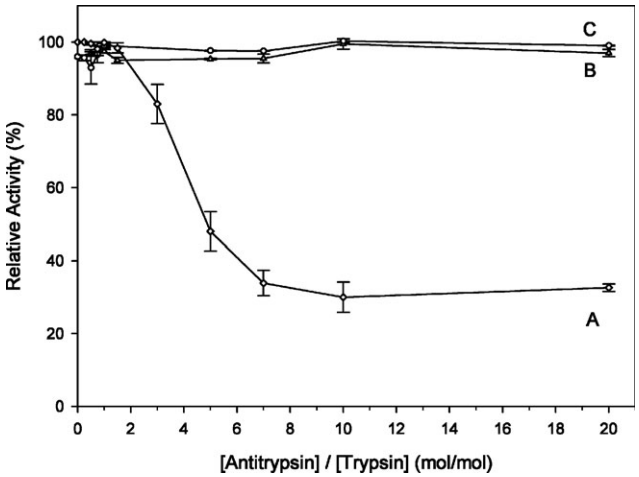

Fig. 7 Relative activity of free (A) and conjugated trypsin microspheres, P(S-DVB)/PAA2-GA-trypsin (B) and P(S-DVB)/PVBA-Trypsin (C), as a function of [antitrypsin]/[trypsin] mol ratio. The trypsin-conjugated microspheres and the inhibition with α_1-antitrypsin were performed according to the Experimental section. Activity measurements against BAEE were also accomplished according to the Experimental section.

7. At a ratio of 7, the activity loss was approximately 70%. However, curves A and B in Fig. 7 demonstrate that the trypsin bound to the P(S-DVB)/PAA-GA and P(S-DVB)/PVBA microspheres retained almost all of its activity even at a [antitrypsin]/[trypsin] mol ratio higher than 20.

Summary and conclusions

This study demonstrates a simple and convenient method for the functionalization of crosslinked P(S-DVB) microspheres by ozonolysis. The ozone treatment of these particles promotes the formation of various oxygen-containing groups, *e.g.* carbonyls, carboxyls, hydroxyls and hydroperoxides. The redox graft polymerization of vinylic monomers such as AN and CMS on the P(S-DVB) microspheres was performed at room temperature by the conjugated hydroperoxides/$NaHSO_3$ redox pair initiator. The main conclusions arising out of this study are as follows.

(1) A 1 : 1 mol ratio of [$NaHSO_3$] : [conjugated hydroperoxides] was not sufficient for the efficient graft polymerization of AN or CMS. The optimal mol ratios were 10 : 1 for AN and CMS. Using a $NaHSO_3$ concentration above this ratio resulted in a lower grafting yield, probably due to chain termination processes.

(2) The % grafting yield of PAN and PCMS on the P(S-DVB) microspheres rose as the concentration of the conjugated hydroperoxides increased. However, above a certain concentration, the % grafting yield did not change significantly.

(3) The decomposition temperature of the P(S-DVB) rose as the PAN content of the P(S-DVB)/PAN composite particles increased.

(4) The redox graft polymerization of AN and CMS on the P(S-DVB) microspheres occurred on both the inner pores and the outer surface of the particles. Under similar polymerization conditions the PCMS grafting yield was significantly higher than that of the PAN.

(5) The activity towards BAEE of P(S-DVB)/PAA-GA-Trypsin microspheres was significantly higher than that of P(S-DVB)/PVBA-Trypsin in spite of the fact that the trypsin content of the first type of the polyaldehyde particles was approximately two-fold lower than that of the other ones.

(6) Covalent immobilization of trypsin to the polyaldehyde particles resulted in decreasing activity against BAEE and increasing stability against the inhibitor α_1-antitrypsin.

In future work we wish to extend these studies to particles of lower diameters, *e.g.* below 100 nm, and to the graft polymerization of other vinylic monomers such as acrolein and acrylic acid. The optimal systems will then be used for various applications, *e.g.* coupling of different bioactive amino ligands (proteins, antibodies, enzymes, *etc.*) to the functional particles, *via* different activation methods, for biomedical applications,[3,7] and the synthesis of carbon nano- and micron-sized particles by carbonization of the PAN grafted particles.

Acknowledgements

These studies were partially supported by a Minerva Grant (Microscale & Nanoscale Particles and Films) and by The Israeli Ministry of Commerce & Industry (NFM Consortium on Nanoparticles for Industrial Applications).

References

1 R. Arshady, S. Margel, C. Pichot and T. Delair, *Microspheres, Microcapsules Liposomes*, 1999, **1**, 165–195.
2 S. Margel, E. Nov and I. Fisher, *J. Polym. Sci., Part A: Polym. Chem.*, 1991, **29**, 347–355.
3 S. Margel, S. Sturchak, E. Ben-Bassat, A. Reznikov, B. Nitzan, R. Krasniker, O. Melamed, M. Sadeh, S. Gura, E. Mandel, E. Michael and I. Burdygine, *Microspheres, Microcapsules Liposomes*, 1999, **2**, 11–42.
4 J. W. Vanderhoff, M. S. El-Aasser, F. J. Micale, E. D. Sudol, C. M. Tseng, A. Silwanowicz, H. R. Sheu and D. M. Kornfeld, *Polym. Mater. Sci. Eng.*, 1986, **54**, 587–592.
5 J. Ugelstad, A. Berge, T. Ellingsen, R. Schmid, T. N. Nilsen, P. C. Moerk, P. Stenstad, E. Hornes and O. Olsvik, *Prog. Polym. Sci.*, 1992, **17**, 87–161.
6 *Polymeric Dispersions: Principles and Applications*, ed. J. M. Asua, Elizondo, Spain, 1997.
7 S. Margel, I. Burdygin, V. Reznikov, B. Nitzan, O. Melamed, M. Kedem, S. Gura, G. Mandel, M. Zuberi and L. Boguslavsky, *Recent Res. Dev. Polym. Sci.*, 1997, **1**, 51–78.
8 H. Bamnolker and S. Margel, *J. Polym. Sci., Part A: Polym. Chem.*, 1996, **34**, 1857–1871.
9 Y. Almog, S. Reich and M. Levy, *Br. Polym. J.*, 1982, **14**, 131–136.
10 A. J. Paine, *Macromolecules*, 1990, **23**, 3109–3117.
11 J.-W. Kim and K.-D. Suh, *Polymer*, 2000, **41**, 6181–6188.
12 K. Li and H. D. H. Stover, *J. Polym. Sci., Part A: Polym. Chem.*, 1993, **31**, 2473–2479.
13 J. S. Downey, R. S. Frank, W.-H. Li and H. D. H. Stoever, *Macromolecules*, 1999, **32**, 2838–2844.
14 W.-H. Li and H. D. H. Stover, *J. Polym. Sci., Part A: Polym. Chem.*, 1998, **36**, 1543–1551.
15 W.-H. Li, K. Li and H. D. H. Stover, *J. Polym. Sci., Part A: Polym. Chem.*, 1999, **37**, 2295–2303.
16 W.-H. Li and H. D. H. Stoever, *Macromolecules*, 2000, **33**, 4354–4360.
17 J. Ugelstad, *Makromol. Chem.*, 1978, **179**, 815–817.
18 J. Ugelstad, P. C. Moerk, K. Herder Kaggerud, T. Ellingsen and A. Berge, *Adv. Colloid Interface Sci.*, 1980, **13**, 101–140.

19 C. M. Cheng, F. J. Micale, J. W. Vanderhoff and M. S. El-Aasser, *J. Polym. Sci., Part A: Polym. Chem.*, 1992, **30**, 235–244.
20 K. Hosoya and J. M. J. Frechet, *J. Polym. Sci., Part A: Polym. Chem.*, 1993, **31**, 2129–2141.
21 V. Smigol, F. Svec, K. Hosoya, Q. Wang and J. M. J. Frechet, *Angew. Makromol. Chem.*, 1992, **195**, 151–164.
22 V. Smigol and F. Svec, *J. Appl. Polym. Sci.*, 1992, **46**, 1439–1448.
23 Y.-C. Liang, F. Svec and J. M. J. Frechet, *J. Polym. Sci., Part A: Polym. Chem.*, 1997, **35**, 2631–2643.
24 M. Okubo, E. Ise and T. Yamashita, *J. Appl. Polym. Sci.*, 1999, **74**, 278–285.
25 M. Okubo and M. Shiozaki, *Polym. Int.*, 1993, **30**, 469–474.
26 M. Kedem and S. Margel, *J. Polym. Sci., Part A: Polym. Chem.*, 2002, **40**, 1342–1352.
27 B. C. Bunker, P. C. Rieke, B. J. Tarasevich, A. A. Campbell, G. E. Fryxell, G. L. Graff, L. Song, J. Liu, J. W. Virden and G. L. McVay, *Science*, 1994, **264**, 48–55.
28 S. Margel, E. A. Vogler, L. Firment, T. Watt, S. Haynie and D. Y. Sogah, *J. Biomed. Mater. Res.*, 1993, **27**, 1463–1476.
29 D. J. Carlsson and D. M. Wiles, *J. Macromol. Sci., Rev. Macromol. Chem.*, 1976, **C14**, 65–106.
30 R. D. Badley, W. T. Ford, F. J. McEnroe and R. A. Assink, *Langmuir*, 1990, **6**, 792–801.
31 J.-W. Byun and Y.-S. Lee, *J. Ind. Eng. Chem. (Seoul)*, 2004, **10**, 283–289.
32 J. Lacoste, D. Vaillant and D. J. Carlsson, *J. Polym. Sci., Part A: Polym. Chem.*, 1993, **31**, 715–722.
33 H. Ichijima, T. Okada, Y. Uyama and Y. Ikada, *Makromol. Chem.*, 1991, **192**, 1213–1221.
34 E. A. Kulik, M. I. Ivanchenko, K. Kato, S. Sano and Y. Ikada, *J. Polym. Sci., Part A: Polym. Chem.*, 1995, **33**, 323–330.
35 P. Gatenholm, T. Ashida, Y. Nabeshima and A. S. Hoffman, *Polym. Mater. Sci. Eng.*, 1992, **66**, 445–446.
36 S. D. Razumovskii and G. E. Zaikov, *Ozone and Its Reactions with Organic Compounds*, Elsevier, Amsterdam, 1984.
37 E. Partouche, D. Waysbort and S. Margel, *J. Colloid Interface Sci.*, 2006, **294**, 69–78.
38 S. Margel and E. Wiesel, *J. Polym. Sci., Polym. Chem. Ed.*, 1984, **22**, 145–158.
39 S. Margel, *J. Polym. Sci., Polym. Chem. Ed.*, 1984, **22**, 3521–3533.
40 S. Margel, *J. Chromatogr., A*, 1989, **462**, 177–189.
41 S. D. Razumovskii, O. N. Karpukhin, A. A. Kefeli, T. V. Pokholok and G. E. Zaikov, *Vysokomol. Soedin., Ser. A*, 1971, **13**, 782–790.
42 K. Matsumoto, R. Izumi, H. Seijo and H. Mizuguchi, *US Pat.*, 4486549, 1984.
43 S. J. Angyal, *Org. React.*, 1954, 197–217.
44 D. J. Carlsson and D. M. Wiles, *Macromolecules*, 1969, **2**, 597–606.
45 V. K. Sarin, S. B. Kent, J. P. Tam and R. B. Merrifield, *Anal. Biochem.*, 1981, **117**, 147–157.
46 E. Kaiser, R. L. Colescott, C. D. Bossinger and P. I. Cook, *Anal. Biochem.*, 1970, **34**, 595–598.
47 O. H. Lowry, N. J. Rosebrough, A. L. Farr and R. J. Randall, *J. Biol. Chem.*, 1951, **193**, 265–275.
48 *The Enzymes, Vol. 3: Hydrolysis: Peptide Bonds*, ed. P. D. Boyer, Academic, New York, 3rd edn, 1971.
49 R. J. Hunter, *Introduction to Modern Colloid Science*, Oxford University Press, Oxford, 1993.
50 L. Boguslavsky and S. Margel, *J. Polym. Sci., Part A: Polym. Chem.*, 2004, **42**, 4847–4861.
51 B. C. Oxenrider,F. Mares and M. S. Yang, *US Pat.*, 5453477, 1995.
52 D. J. Lamb, C. M. Fellows and R. G. Gilbert, *Polymer*, 2005, **46**, 7874–7895.
53 U. D. N. Bajpai, A. K. Bajpai and J. Bajpai, *J. Indian Chem. Soc.*, 1992, **69**, 841–845.
54 J. R. Ebdon, T. N. Huckerby and T. C. Hunter, *Polymer*, 1994, **35**, 250–256.
55 J. E. McGrath, *J. Chem. Educ.*, 1981, **58**, 844–861.
56 Z. Bashir, *Carbon*, 1991, **29**, 1081–1090.
57 S. Margel, L. Sheihet and T. Tennenbaum, *Int. Pat.*, WO 45494 A2, June 3 Pat., 2004/045494 A2, 2004.
58 D. Goradia, J. Cooney, B. K. Hodnett and E. Magner, *J. Mol. Catal. B: Enzym.*, 2005, **32**, 231–239.

